Bulletin of the Seismological Society of America, Vol. 97, No. 6, pp. 2152–2170, December 2007, doi: 10.1785/0120070081

The Influence of Magnitude Range on Empirical Ground-Motion Prediction

by Julian J. Bommer*, Peter J. Stafford, John E. Alarcón, and Sinan Akkar

Abstract A key issue in the assessment of seismic hazard in regions of low-to-moderate seismicity is the extent to which accelerograms obtained from small-magnitude earthquakes can be used as the basis for predicting ground motions due to the larger-magnitude events considered in seismic hazard analysis. In essence, the question is whether empirical ground-motion prediction equations can be applied outside their strict range of applicability as defined by the magnitude and distance ranges covered by the datasets from which they are derived. This question is explored by deriving new spectral prediction equations using an extended strong-motion dataset from Europe and the Middle East covering the magnitude range M_w 3.0–7.6 and comparing the predictions with previous equations derived using data from only M_w 5.0 and above events. The comparisons show that despite their complex functional form, including quadratic magnitude-dependence and magnitude-dependent attenuation, the equations derived from larger-magnitude events should not be extrapolated to predict ground motions from earthquakes of small magnitude. Moreover, the results suggest not only that ground-motion prediction equations cannot be used outside the ranges of their underlying datasets but also that their applicability at the limits of these ranges may be questionable. Although only tested for smaller magnitudes, the results could be interpreted to suggest that predictive equations also cannot be reliably extrapolated to higher magnitudes than those represented in the dataset from which they are derived, a finding that has important implications for seismic hazard analysis.

The conclusion of the study is that empirical derivation of ground-motion prediction equations should be based on datasets extending at least one unit below the lower limit of magnitude considered in seismic hazard calculations. The inclusion of small-magnitude recordings results in a significant increase in the aleatory variability of the equations, although it is yet to be established whether this is due to greater uncertainty in the associated metadata or whether ground-motion variability is genuinely dependent on earthquake magnitude.

Introduction

The smallest earthquakes for which there are reliable reports of appreciable damage to the built environment have had moment magnitudes slightly greater than M_w 5 (Bommer *et al.*, 2001). Consequently, the focus of engineering seismology has been primarily on moderate-to-large events, except for special circumstances such as consideration of the hazard and risk posed by induced seismicity (e.g., Bommer *et al.*, 2006; van Eck *et al.*, 2006). Probabilistic seismic hazard analysis (PSHA) imposes a lower magnitude limit on the integrations across scenarios in order to exclude contributions to the hazard associated with high-frequency ground-motion amplitudes from earthquakes considered to be too small to be of relevance to engineering design. This is reflected in the ranges of magnitude covered by the strong-motion datasets used for the derivation of empirical ground-motion prediction equations: the vast majority of equations derived for western North America since 1981 have had a lower magnitude limit (using various scales) of 5.0 (Douglas, 2003a). Whereas in other parts of the world, such as Europe, some equations have been derived using data from earthquakes of magnitude 4 and above (e.g., Ambraseys *et al.* [1996] using M_S), recent equations in this region have also adopted the lower limit of M_w 5 (Ambraseys *et al.*, 2005; Akkar and Bommer, 2007a,b). Some other studies, how-

*Corresponding author; j.bommer@imperial.ac.uk.

ever, have derived equations from datasets based entirely on recordings of small-to-moderate magnitude earthquakes (Theodulidis, 1998; Bragato and Slejko, 2005; Frisenda *et al.*, 2005). These studies have all concluded that equations derived from larger-magnitude earthquake recordings systematically overestimate the ground motions produced by smaller-magnitude events. Dost *et al.* (2004) reached a similar conclusion in exploring the ability of widely used empirical equations to estimate the peak accelerations and velocities recorded from small-magnitude events in The Netherlands.

The discrepancies between ground-motion prediction equations derived from small- and large-magnitude recordings have recently been explored by F. Cotton *et al.* (unpublished manuscript, 2007) using Kik-net data from Japan. This study concludes that the differences are due to two factors: motions from smaller-magnitude recordings decay more rapidly, and magnitude scaling of ground-motion amplitudes decreases with increasing magnitude. Some other studies, however, have compared the predictions from equations derived using recordings from moderate-to-large magnitude events with recordings from small-to-moderate events and have concluded that the overestimation of the latter by the former is due, amongst other explanations, to regional differences in ground motions (e.g., Marin *et al.*, 2004). The issue is of great importance in PSHA for safety-critical projects such as nuclear power plants in regions of low-to-moderate seismicity where there are only strong-motion recordings of relatively small events, as is the case, for example, in Central Europe (Cotton *et al.*, 2006). Scherbaum *et al.* (2004) found that the only region-specific equation for Central Europe, derived from small-magnitude events, provided poorer predictions of recordings from the M_w 4.8 St. Dié earthquake of February 2003 than many equations from other regions.

In this study, we explore the issue of extrapolating ground-motion predictions from small-to-large magnitude earthquakes by performing a simple experiment in the opposite direction. A strong-motion dataset covering magnitudes from M_w 5.0 to 7.6 has recently been used to derive equations for the prediction of response spectral ordinates in Europe and the Middle East (Akkar and Bommer, 2007b). The dataset is extended to include recordings from earthquakes as small as M_w 3.0, and new equations are derived using exactly the same functional form and regression techniques. The predictions from the two sets of equations, nominally valid for different magnitude ranges, are then compared, particularly for small magnitudes where only the new equations are constrained by the data.

Data and Regression Analysis

Akkar and Bommer (2007b) present equations for the prediction of response spectral ordinates at periods from 0.0 to 4.0 sec, for damping ratios of 2%, 5%, 10%, 20%, and 30% of critical, derived from strong-motion accelerograms from Europe and the Middle East. The dataset, which is essentially the same as that used by Ambraseys *et al.* (2005), consists of 532 recordings obtained at distances up to 100 km from 131 earthquakes with magnitudes ranging from M_w 5.0 to 7.6. The characteristics of the strong-motion data set are presented together with predictive equations for peak ground velocity (PGV) in Akkar and Bommer (2007a). In the same paper, the selection of the following functional form for the equations is also presented:

$$\log_{10}[\mathrm{PSA}(T)] = b_1 + b_2 M_w + b_3 M_w^2 + (b_4 + b_5 M_w)\log_{10}\sqrt{R_{jb}^2 + b_6^2} + f(S,F), \quad (1)$$

where $f(S,F) = b_7 S_S + b_8 S_A + b_9 F_N + b_{10} F_R$, in which $\mathrm{PSA}(T)$ is the geometric mean of the two horizontal components of 5%-damped pseudospectral acceleration in units of cm/sec^2 (and T is the period in sec); R_{jb} is the Joyner–Boore distance (see Abrahamson and Shedlock, 1997) in km; S_S and S_A are dummy variables taking values of 1 for soft soil ($V_{s30} < 360$ m/sec) and stiff soil ($360 < V_{s30} < 750$ m/sec), respectively, and are 0 otherwise; and F_N and F_R are similar variables taking a value of unity for normal and reverse faulting events, respectively, and are 0 otherwise.

The European Strong-Motion Database (Ambraseys *et al.*, 2004) was searched for events smaller than M_w 5.0 obtained at distances of 100 km or less, for which site classification of the recording stations and the style of faulting—as defined by Akkar and Bommer (2007a)—for the causative rupture were available. The smallest event for which a record was found was M_w 2.0, but only 11 accelerograms were retrieved from earthquakes smaller than M_w 3.0 and so this was taken as the lower limit. A total of 465 records from 158 earthquakes were added to the dataset, bringing the total database for the regressions to 997 recordings from 289 events.

The basic information on the earthquakes generating these records is presented in Table 1, and the distribution of the data with respect to magnitude, distance, and site classification is presented in Figure 1. Although equation (1) is defined in terms of the Joyner–Boore distance, for these small-magnitude recordings only epicentral distances are available, but for events smaller than M_w 5.0, the two distance metrics can be considered equivalent by virtue of the small dimensions of the fault ruptures.

The data can be seen to be well distributed with respect to magnitude, distance, and site classification, although for $M_w < 4.0$ the data are sparse at distances greater than 40 km. Seventy-five recordings are from soft-soil sites, 173 are from stiff-soil sites, and the remaining 217 are from rock sites. The distribution with respect to the style of faulting is less even, with just 24 records from reverse earthquakes, 140 from strike-slip earthquakes, and the remaining 291 from normal ruptures. This means that the uneven distribution among the styles of faulting is exaggerated in the extended magnitude

Table 1

Characteristics of $M_w < 5$ Earthquakes Contributing Records to the Extended Database

Earthquake Country	Earthquake ID	Number of Recordings	Year	Month	Day	M_w	Mechanism	Earthquake Country	Earthquake ID	Number of Recordings	Year	Month	Day	M_w	Mechanism
Italy	62	1	1976	9	13	4.8	R	Spain	1146	2	1997	7	2	3.9	S
Italy	64	2	1976	9	15	4.9	R	Spain	1147	4	1997	7	3	4	S
Germany	68	1	1977	2	11	3.6	S	Spain	1153	2	1997	8	20	4	R
Germany	77	1	1978	1	16	3.1	S	Spain	1159	1	1997	10	13	3.8	S
Germany	78	1	1978	1	16	3.3	S	Switzerland	1164	3	2000	3	4	3.6	R
Germany	79	1	1978	2	6	3.2	S	Switzerland	1165	7	2000	4	6	4.1	N
Germany	88	1	1978	9	19	3.2	S	Germany	1175	1	1983	9	11	3.1	S
Germany	123	1	1980	4	21	3.2	S	Germany	1176	1	1982	11	28	3.2	S
Italy	178	6	1984	5	11	4.7	N	Switzerland	1543	1	2000	11	13	3.2	S
Italy	179	6	1984	5	11	4.8	N	Switzerland	1623	6	2001	2	23	3.5	S
Italy	181	4	1984	5	11	4.8	N	Switzerland	1624	2	2001	2	25	3.3	S
Greece	194	1	1986	9	13	4.1	N	Switzerland	1630	1	2001	3	17	3.4	S
Greece	196	1	1986	9	14	3.9	N	Saudi Arabia	1659	1	1995	12	2	4.1	N
Greece	197	4	1986	9	15	4.9	N	Switzerland	1702	1	1996	2	21	3.1	S
Greece	198	1	1986	9	15	4.1	N	Egypt	1879	1	1995	12	26	4.5	S
Greece	202	1	1988	4	24	4.8	R	Greece	1890	1	1997	2	22	4.2	N
Greece	205	1	1988	7	5	4.9	N	Greece	1894	1	1997	10	21	4.7	N
Greece	209	1	1988	9	30	4.7	S	Greece	1903	1	1997	4	29	4.5	R
Greece	217	2	1988	12	22	4.9	N	Greece	1904	1	1997	11	18	4.8	R
Greece	223	2	1989	8	31	4.8	N	Greece	1905	1	1997	11	19	4.8	R
Greece	265	2	1993	3	26	4.9	S	Greece	1909	1	1996	7	27	4.3	N
Greece	266	2	1993	3	26	4.9	S	Greece	1913	3	1996	12	5	4.2	N
Greece	269	2	1993	3	26	4.7	S	Greece	1915	1	1996	8	11	4.7	S
Greece	277	3	1993	7	14	4.6	S	Greece	2032	1	1995	5	14	4.5	N
Greece	278	1	1993	7	14	4.6	S	Greece	2034	1	1995	5	16	4.7	N
Greece	283	3	1994	2	27	4.8	R	Greece	2035	2	1995	5	16	4.9	N
Switzerland	285	9	1998	5	7	3.1	N	Greece	2038	1	1995	5	18	4.6	N
Italy	287	3	1997	9	3	4.5	N	Greece	2039	5	1995	6	6	4.2	N
Spain	307	1	1984	6	24	4.9	N	Greece	2040	6	1995	6	11	4.8	N
France	346	3	1996	7	15	4.2	S	Greece	2042	1	1995	5	15	4.4	N
Spain	348	7	1994	1	4	4.9	N	Greece	2043	1	1995	5	15	3.6	N
Italy	351	5	1997	10	4	4.7	N	Greece	2044	1	1995	5	15	3.8	N
Italy	352	6	1997	10	7	4.2	N	Greece	2045	1	1995	5	15	4.4	N
Italy	353	8	1997	10	7	4.5	N	Greece	2046	1	1995	5	16	4.8	N
Italy	358	9	1997	10	16	4.3	S	Greece	2048	1	1995	5	30	3.5	N
Italy	360	9	1997	11	9	4.9	N	Greece	2049	1	1995	7	18	4.3	N
Italy	365	13	1998	4	5	4.8	N	Greece	2051	1	1995	5	21	4.1	N
Italy	367	3	1997	10	13	4.4	N	Greece	2053	1	1995	7	18	4.7	N
Italy	477	20	1996	3	31	4.2	N	Greece	2054	1	1995	5	22	3.1	N
Switzerland	484	1	1999	2	14	4	S	Greece	2055	1	1995	5	23	4.4	N
Germany	488	22	1992	12	30	3.7	S	Greece	2057	2	1995	4	4	4.6	N
Switzerland	495	1	1989	9	30	3.9	S	Greece	2058	2	1995	5	3	4.7	N
Switzerland	508	7	1996	8	24	3.8	N	Greece	2059	2	1995	5	3	4.6	N
Switzerland	511	3	1998	4	21	3.4	S	Greece	2060	2	1995	5	3	4.7	N
Germany	529	1	1996	6	28	3	S	Greece	2064	1	1986	9	13	3.8	N

Table 1 (*Continued*)

Earthquake Country	Earthquake ID	Number of Recordings	Year	Month	Day	M_w	Mechanism	Earthquake Country	Earthquake ID	Number of Recordings	Year	Month	Day	M_w	Mechanism
Switzerland	538	1	1998	12	9	3.3	N	Greece	2065	1	1995	5	19	4.8	N
Switzerland	540	1	1995	10	7	3.3	S	Greece	2066	2	1995	5	20	4.3	S
Switzerland	542	1	1995	9	17	3.5	S	Greece	2067	1	1995	6	8	4.4	N
Switzerland	555	1	1997	10	23	3	S	Greece	2068	1	1995	8	20	4.2	N
Switzerland	556	1	1999	9	12	3	S	Greece	2069	1	1995	8	20	3	N
France	558	1	1980	7	15	4.9	S	Greece	2070	1	1995	11	15	3.8	N
Greece	610	1	1995	8	13	4.5	N	Greece	2071	1	1995	5	13	4.4	N
Greece	623	3	1995	6	25	4.1	N	Greece	2073	1	1995	5	13	4.6	N
Greece	635	1	1983	2	20	4.9	S	Greece	2074	1	1988	10	17	4.4	S
Greece	649	2	1987	1	31	4.1	N	Greece	2078	1	1995	4	4	4.3	N
Greece	650	1	1988	4	3	4.5	N	Greece	2079	1	1995	5	7	3.9	N
Greece	656	1	1988	10	20	4.2	S	Greece	2143	2	2001	4	8	4.2	N
Greece	663	2	1983	6	14	4.4	S	Turkey	2158	8	1999	11	7	4.9	R
Greece	668	1	1989	5	15	4.8	N	Italy	2169	2	2001	7	17	4.8	S
Greece	670	1	1993	2	14	4.5	S	Italy	2173	1	2001	10	1	3.8	N
Greece	671	1	1993	2	15	4.1	S	Italy	2178	1	2002	1	18	3.3	N
Greece	672	1	1993	3	25	4.5	S	France	2198	1	2001	2	25	4.5	R
Greece	673	1	1993	3	26	4.5	S	Italy	2200	2	1997	9	26	4.5	N
Greece	674	1	1993	4	29	4.8	S	Italy	2202	4	1997	9	27	4.4	N
Greece	675	1	1988	6	11	4.2	S	Italy	2209	1	1997	10	16	3.9	N
Greece	685	1	1988	10	23	4.3	S	Italy	2211	5	1997	10	19	4.2	N
Greece	701	1	1980	9	26	4.8	N	Italy	2214	7	1998	2	7	4.4	N
Greece	718	1	1988	10	28	4.4	S	Italy	2217	6	1998	4	3	4.3	N
Switzerland	989	12	1999	12	29	4.9	N	Turkey	2223	1	2000	9	8	4.6	S
Italy	990	8	1999	12	31	4.1	N	Turkey	2297	1	2002	10	17	4.7	S
Switzerland	993	5	1999	12	29	3	N	France	2389	4	2003	2	22	4.7	S
Turkey	1015	4	1999	8	29	4.2	N	Switzerland	2394	2	2003	2	4	3.1	N
Switzerland	1021	6	2000	2	23	3.1	S	Switzerland	2403	13	2003	4	29	3.5	S
Spain	1079	1	1996	2	18	4.4	S	Switzerland	2404	2	2003	5	6	3.6	S
Spain	1107	3	1996	9	2	4.4	N	Switzerland	2406	3	2003	7	17	3.5	N
Spain	1113	16	1996	12	28	3.9	N	Switzerland	2407	3	2003	7	18	3.5	N
Spain	1114	19	1997	2	24	4.2	N	Italy	2411	1	2002	4	29	3.5	S
Spain	1144	7	1997	7	2	4.5	S	Switzerland	2412	5	2003	8	1	3.7	S
Spain	1145	9	1997	7	2	4.4	S	Georgia	2498	1	2002	4	25	4.8	S

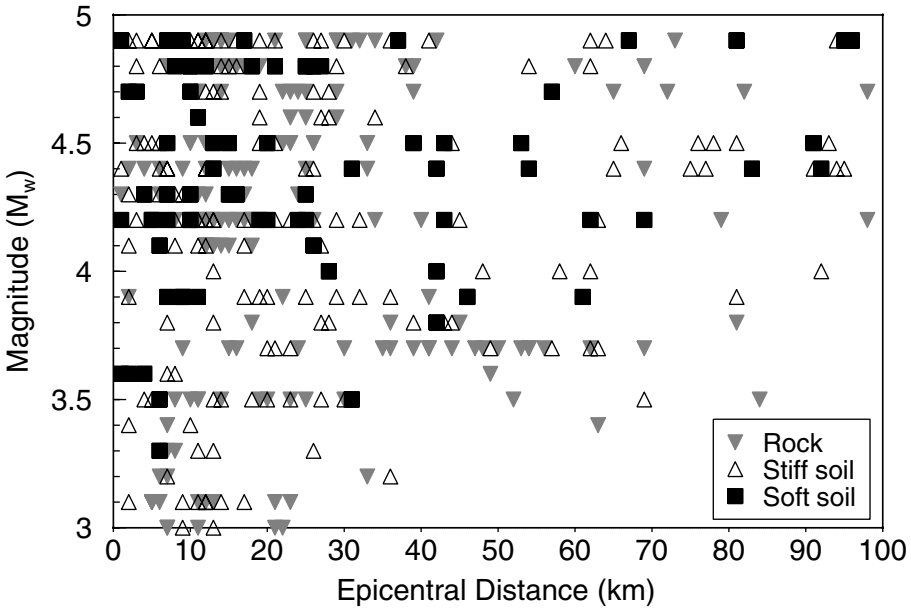

Figure 1. Magnitude–distance distribution of small-magnitude recordings added to the dataset; symbols indicate the site classification.

range dataset; whereas for the larger events used by Akkar and Bommer (2007b) reverse faulting earthquakes were responsible for about 18% of the total, in the extended dataset they account for just 12% of the recordings.

Examination of Table 1 can give the impression that the additional data is predominantly from Greece, which might represent a regional bias in the data. However, although there are a large number of Greek earthquakes contributing recordings to the smaller-magnitude data, these events are mostly associated with just one or two accelerograms. Figure 2 shows the geographical distribution of the data; it may be appreciated that the distribution of the extended dataset is not particularly different from that of the original dataset of Akkar and Bommer (2007b) except for the addition of recordings from four countries of low-to-moderate seismicity (France, Germany, Spain, and Switzerland) and the inclusion of far fewer records from the most active countries (Iran, Turkey).

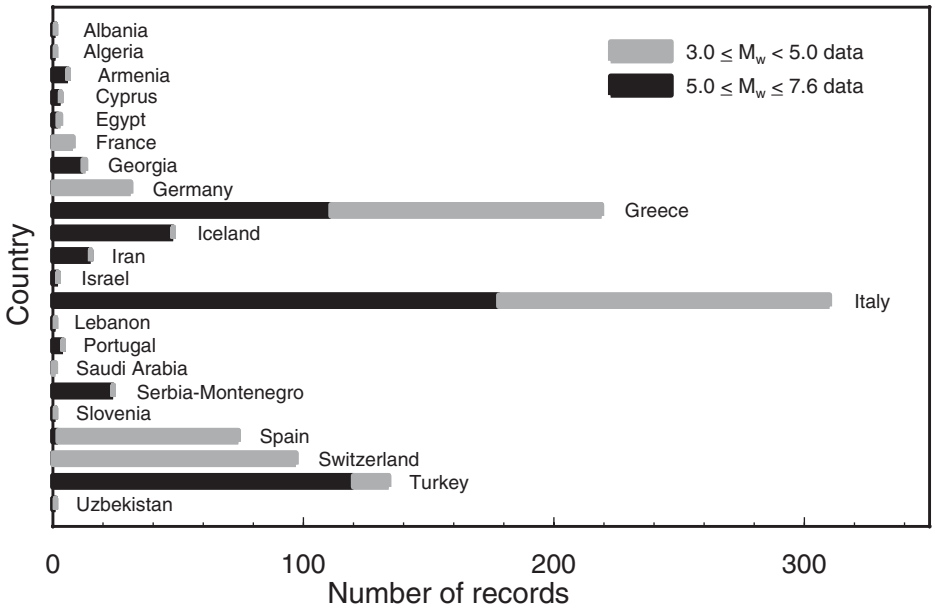

Figure 2. Geographical origin of the extended dataset.

Akkar and Bommer (2007b) developed equations for the prediction of spectral ordinates at response periods up to 4.0 sec by carefully reprocessing the strong-motion accelerograms and applying consistent criteria regarding the usable period range of the filtered records (Akkar and Bommer, 2006); the number of usable records consequently decreased with the increasing response period, and beyond 4.0 sec the number of records was considered insufficient to reliably constrain the regressions. The additional records from smaller-magnitude events were adopted as processed routinely for the European Strong-Motion Database, which means that they were filtered with a low-frequency cutoff at 0.25 Hz. On this basis it was decided that spectral ordinates at periods up to 0.5 sec could be reliably calculated, and because the new equations are derived purely for comparative purposes, this period range was considered sufficient. The usable period range of the data could easily be extended to 2 sec, but it is not the purpose of this study to provide new equations for application; for exploring the influence of extending the lower magnitude limit on the predictions, the short-period motions are of most relevance. Regressions on equation (1) were performed using the complete extended dataset, following exactly the same procedures as employed by Akkar and Bommer (2007a, b); the resulting coefficients for 5%-damped spectral ordinates and the magnitude-dependent standard deviations are presented in Tables 2 and 3, respectively.

Figure 3 shows examples of median values of the spectral acceleration at 0.5 sec predicted by the new equations, for various combinations of magnitude, distance, style of faulting, and site classification. The plots show that the predictions follow expected patterns, with motions on soft-soil sites being greater than those on stiff-soil sites and similarly those on stiff-soil sites being greater than those on rock. Reverse faulting earthquakes are seen to generate stronger motions than strike-slip and normal ruptures, which produce almost identical motions, as found by Bommer *et al.* (2003). These trends are all consistent with the original equations of Akkar and Bommer (2007b). On the basis of these observations it can be concluded that the new equations are robust and reliable and can be used with confidence to predict ground motions over a wide range of magnitudes.

Comparisons with Equations for Limited Magnitude Ranges

Figure 4 compares the new equation for peak ground acceleration (PGA) with that of Akkar and Bommer (2007b) for M_w 3–7 and for distances up to 100 km. The plot shows that the new equations cap>ture a much stronger nonlinearity

Table 2
Regression Coefficients of Equation (1) Obtained Using the Extended Dataset

T (sec)	b_1	b_2	b_3	b_4	b_5	b_6	b_7	b_8	b_9	b_{10}
0.00	0.0031	1.0848	−0.0835	−2.4423	0.2081	8.0282	0.0781	0.0208	−0.0292	0.0963
0.05	0.4251	1.0246	−0.0793	−2.5379	0.2128	8.1789	0.0425	−0.0075	−0.0385	0.1056
0.10	−0.4749	1.3892	−0.1107	−2.5861	0.2224	8.9151	0.0292	0.0129	−0.0514	0.0985
0.15	−1.4596	1.6752	−0.1298	−2.4580	0.2067	9.0852	0.0269	0.0280	−0.0498	0.0962
0.20	−2.2362	1.8453	−0.1386	−2.3159	0.1909	8.5791	0.0609	0.0294	−0.0319	0.0955
0.25	−2.8890	1.9277	−0.1380	−2.0382	0.1547	7.1914	0.0910	0.0404	−0.0361	0.1002
0.30	−3.3622	2.0013	−0.1391	−1.8741	0.1294	6.7018	0.1132	0.0416	−0.0314	0.1075
0.35	−3.6122	2.0029	−0.1348	−1.7689	0.1148	6.2981	0.1362	0.0578	−0.0163	0.1103
0.40	−3.7495	1.9803	−0.1289	−1.6834	0.1000	6.2095	0.1704	0.0776	−0.0122	0.1175
0.45	−3.8277	1.9645	−0.1263	−1.6849	0.1019	6.1421	0.1928	0.0971	−0.0099	0.1172
0.50	−3.9037	1.9273	−0.1197	−1.6129	0.0904	6.0412	0.2054	0.1140	0.0000	0.1069

Table 3
Intra- and Interevent Components of Aleatory Variability (with Standard Errors)

T (sec)	Intraevent (σ_1)	Interevent (σ_2)
0.00	$0.599(\pm0.041)–0.058(\pm0.008)M_w$	$0.323(\pm0.075)–0.031(\pm0.014)M_w$
0.05	$0.578(\pm0.046)–0.052(\pm0.009)M_w$	$0.330(\pm0.081)–0.030(\pm0.015)M_w$
0.10	$0.642(\pm0.046)–0.063(\pm0.009)M_w$	$0.386(\pm0.077)–0.038(\pm0.015)M_w$
0.15	$0.652(\pm0.049)–0.064(\pm0.009)M_w$	$0.413(\pm0.078)–0.040(\pm0.015)M_w$
0.20	$0.690(\pm0.046)–0.070(\pm0.009)M_w$	$0.420(\pm0.076)–0.043(\pm0.014)M_w$
0.25	$0.630(\pm0.045)–0.059(\pm0.009)M_w$	$0.386(\pm0.074)–0.036(\pm0.014)M_w$
0.30	$0.584(\pm0.051)–0.051(\pm0.010)M_w$	$0.372(\pm0.079)–0.033(\pm0.015)M_w$
0.35	$0.525(\pm0.053)–0.040(\pm0.010)M_w$	$0.346(\pm0.080)–0.026(\pm0.015)M_w$
0.40	$0.471(\pm0.051)–0.030(\pm0.010)M_w$	$0.322(\pm0.075)–0.020(\pm0.014)M_w$
0.45	$0.465(\pm0.053)–0.029(\pm0.010)M_w$	$0.316(\pm0.078)–0.019(\pm0.015)M_w$
0.50	$0.423(\pm0.053)–0.021(\pm0.010)M_w$	$0.293(\pm0.077)–0.014(\pm0.015)M_w$

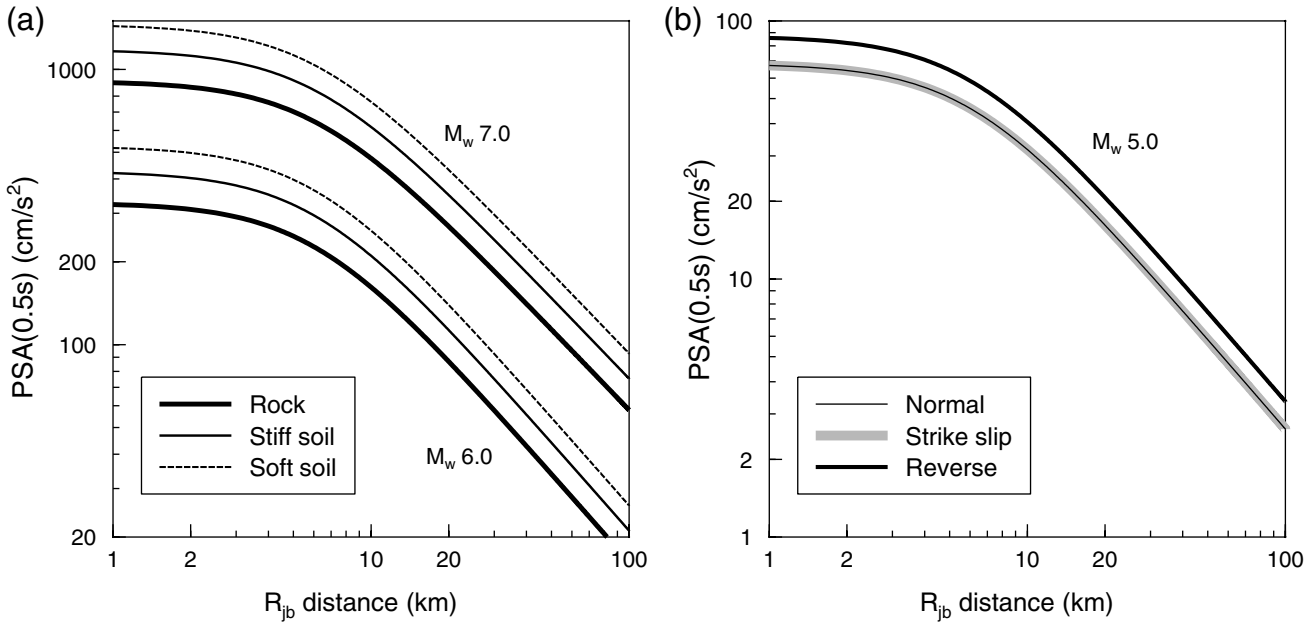

Figure 3. Predicted median values of pseudospectral acceleration at 0.5 sec for different magnitudes against distance. (a) Strike-slip earthquakes and different site classes; (b) rock sites and different styles of faulting

in the magnitude scaling but a much weaker magnitude dependence of the geometric spreading (attenuation).

Figure 5 shows the ratios of median spectral ordinates obtained from the equations of Akkar and Bommer (2007b)

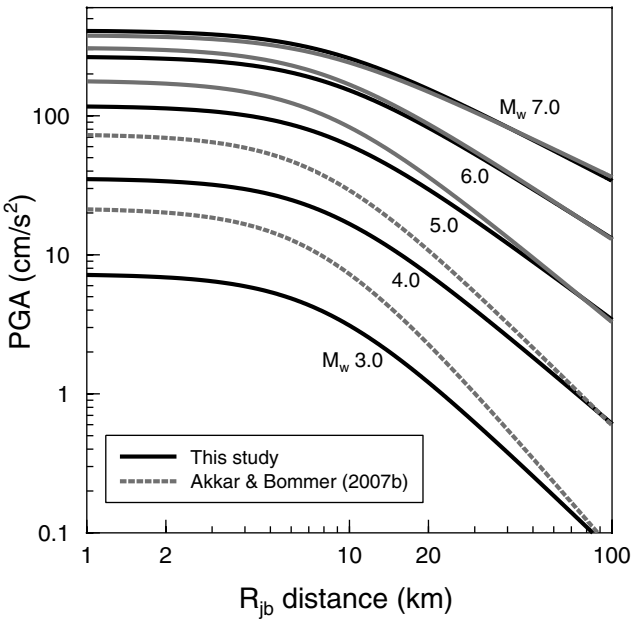

Figure 4. Comparison of predicted median values of PGA for strike-slip ruptures and rock sites from the Akkar and Bommer (2007b) equation and the new equations for extended magnitude range for various combinations of magnitude and distance. The Akkar and Bommer (2007b) values are drawn as dashed lines outside their range of applicability.

and the new coefficients derived using the extended dataset at four response periods for five magnitudes and distances up to 100 km. A number of interesting observations can be made because for M_w 5, 6, and 7 one might expect the equations to predict very similar values. The first and most obvious observation is that for small magnitudes, well beyond the lower limit of applicability of the equations of Akkar and Bommer (2007b), the equations based on larger magnitudes result in gross overestimation of the ground motions. The overestimation decreases with increasing distance from the source, but for the smallest magnitude (M_w 3) over distances of greatest engineering interest (< 25 km), the spectral ordinates are overestimated by factors of between 2 and 13.

This comparison demonstrates very clearly that simply using a functional form that appropriately reflects the nonlinear magnitude scaling and the magnitude dependence of the geometrical spreading does not necessarily mean the resulting equation can be used outside the range covered by the underlying dataset. Indeed, it would seem that unless the dataset itself covers a sufficiently wide range of magnitudes, the scaling and attenuation dependencies are not fully captured.

This leads to the next observation, which is that at magnitude M_w 5, which is the lower limit of the data used by Akkar and Bommer (2007b), the equations do not agree, with the larger-magnitude equations predicting ordinates consistently 1.5 to 2 times greater than the extended range equations. This is interpreted as also being due to the limited magnitude range of the Akkar and Bommer (2007b) equations not allowing the scaling and attenuation dependencies on magnitude to be fully captured. This could be interpreted

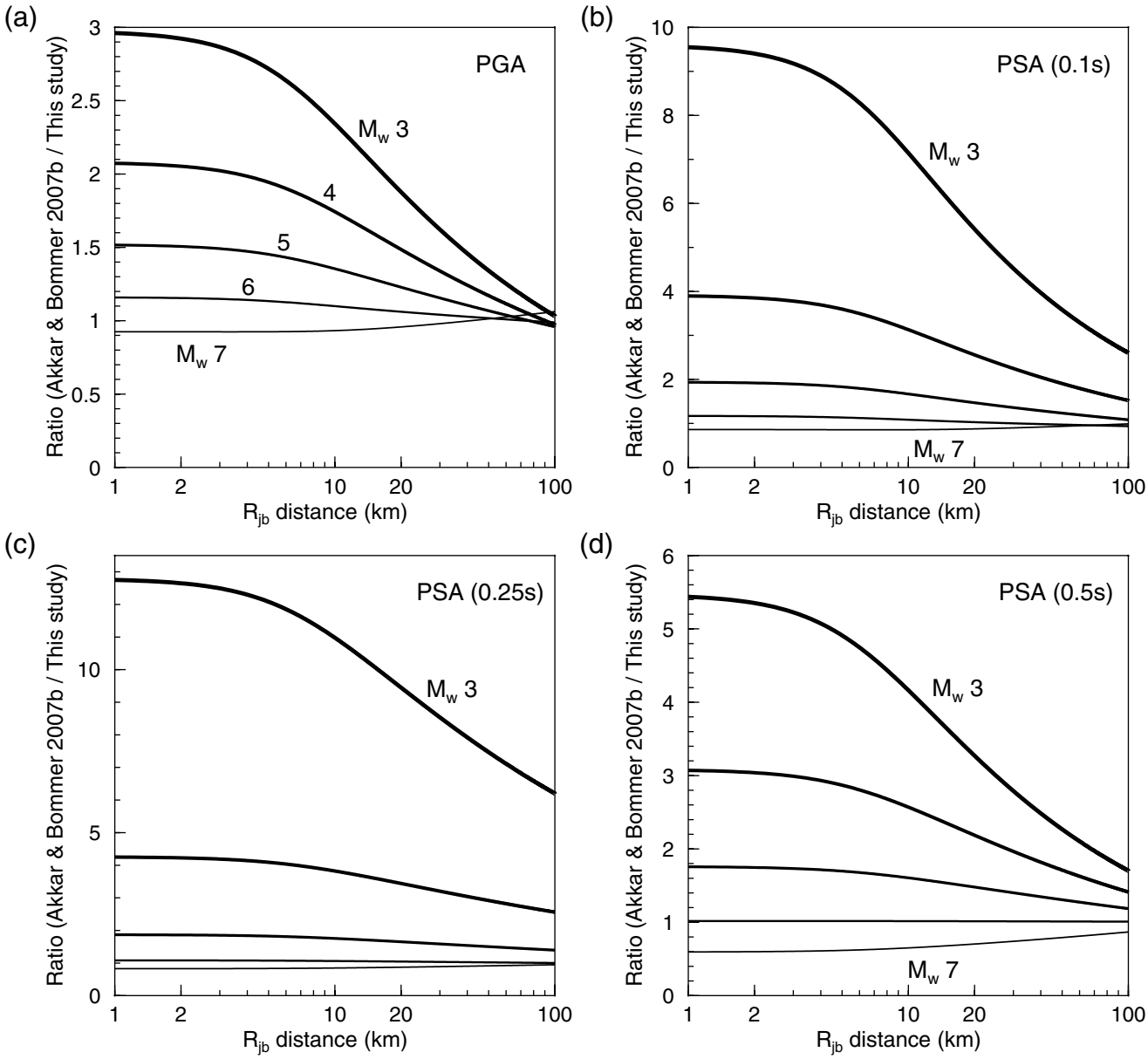

Figure 5. Ratios of spectral ordinates on rock sites at different distances from strike-slip earthquakes of various magnitudes.

as a kind of edge effect, indicating that an empirical equation may not actually be robustly applicable at the limiting magnitude values of the dataset. Figure 6 shows the residuals of records from events in the range M_w 4.9–5.1 compared with the predictions for M_w 5.0 from Akkar and Bommer (2007b) and the new equations. Although the differences are small, the plots do confirm that the equations for which this magnitude is the limiting value of the dataset are less able to predict the motions and in fact tend to overestimate the accelerations.

The troubling implication of this observation is that the same is likely to be true at the upper limit of magnitude, and PSHA very often requires equations to be used for the estimation of ground motions from earthquakes larger than those represented in the dataset. The existence of this edge effect in the upper magnitude range is supported by the fact that at M_w 7 the extended range equations predict higher values than those obtained from Akkar and Bommer (2007b). Additional evidence for edge effects is provided by the fact that for M_w 6, which is well inside the magnitude ranges of both equations, the ratios of predicted ordinates for strike-slip events and rock sites (both of which are well represented in the datasets) are very close to unity.

Figure 7 compares the median 5%-damped response spectral ordinates from the new equations with those from Akkar and Bommer (2007b) and from Bragato and Slejko

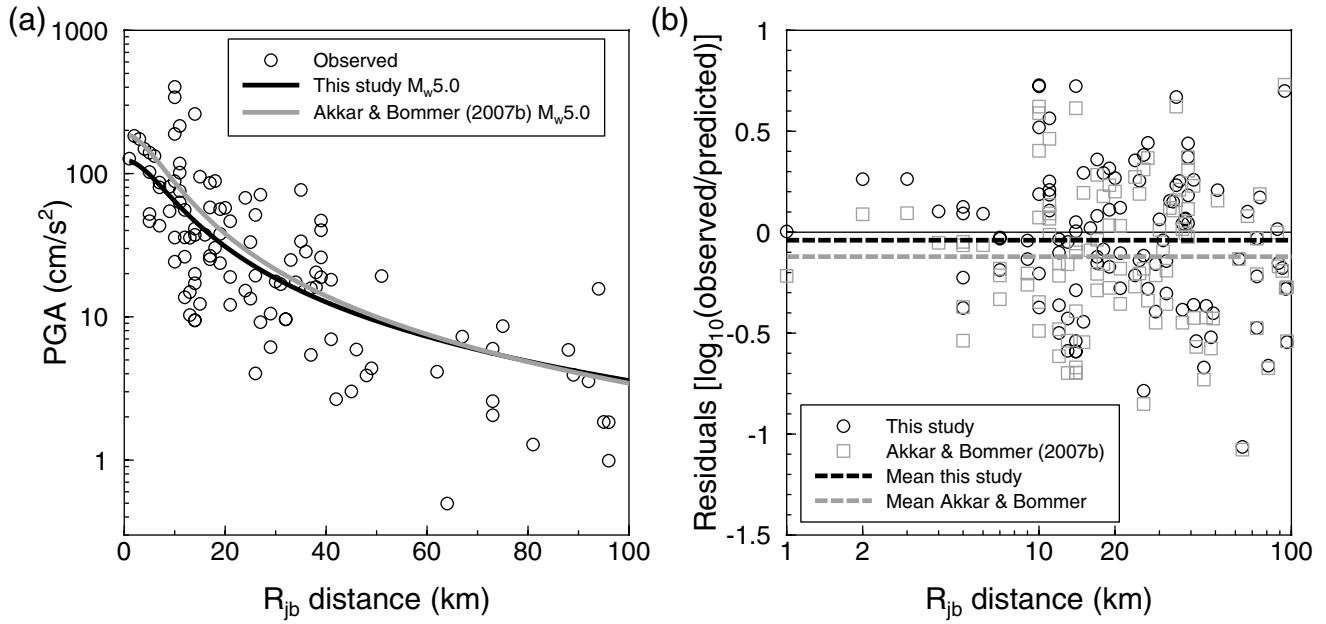

Figure 6. (a) Comparison of recorded PGA values from events of M_w 4.9–5.1 with predictions for M_w 5.0 (for strike-slip rupture and stiff-soil sites) from the equations of Akkar and Bommer (2007b) and the new equation derived for an extended magnitude range; (b) the residuals of the PGA values against distance.

(2005), who used only recordings from earthquakes in northeast Italy with local magnitudes (M_L) from 2.5 to 6.3. While the new equations and those of Akkar and Bommer (2007b) use exactly the same parameter definitions, some adjustments are necessary to achieve compatibility between these equations and those of Bragato and Slejko (2005). The latter equation predicts the maximum vector resultant of the two horizontal components whereas the other two equations predict the geometric mean component. Beyer and Bommer (2006) provide empirical ratios between spectral ordinates using a variety of component definitions, but the vectorally resolved component was not included, so the ratio of 1.27 of this component to the geometric, stipulated by Bragato and Slejko (2005) for PGA, is employed here for the complete spectrum. Bragato and Slejko (2005) use M_L, and it is simply assumed that for small-to-moderate values this scale is equivalent to M_w. All of the equations use Joyner–Boore distance; hence, no adjustments are required for this parameter. We set the predictions from the European equations to reverse faulting, because this is the dominant mechanism in the region from which Bragato and Slejko (2005) obtain their data, and to stiff-soil sites, because Bragato and Slejko (2005) state that this is the class for which their equations are applicable.

In view of the uncertainties associated with generating the plots in Figure 7, the comparisons need to be interpreted with some caution. However, a number of interesting observations can nonetheless be made. The first is that, for magnitudes from M_w 3 to 6, the new equations predict spectral ordinates that are very similar to those from Bragato and Slejko (2005), whereas Akkar and Bommer (2007b) severely overestimate the spectral ordinates except at M_w 6, where all three equations are in broad agreement.

Aleatory Variability

During recent years many empirical ground-motion equations have found that the aleatory variability displays a clear dependency on magnitude in accordance with the observations of Youngs *et al.* (1995). The equations of Ambraseys *et al.* (2005) and Akkar and Bommer (2007a, b) have found magnitude-dependent standard deviations such as those shown in Table 3, confirming the idea that the variability is heteroscedastic with respect to magnitude. For equations covering a wide range of magnitudes, the issue becomes particularly important because if a linear dependence on magnitude is identified, it can result in very broad distributions of the predictions for small magnitudes (Fig. 8).

When extrapolated to small magnitudes, the sigma values become very large, which is important because one of the major advantages of equations for extended magnitude ranges is that they could be used in conjunction with small-magnitude recordings to test the applicability of the equation to a given region following the method of Scherbaum *et al.* (2004). However, if the sigma values are very large, this likelihood approach will not provide a robust indication of the equation's ability to model the data because the equation becomes uninformative regarding its applicability to local data

by virtue of the breadth of the predicted distribution of accelerations.

Additional analyses were conducted to explore the degree to which the apparently very strong variation of the sigma value with magnitude is genuinely supported by the data. The first exercise consisted of testing the sensitivity of the pure error results to the specific binning scheme that was used. The initial pure error results were obtained following the method outlined by Douglas and Smit (2001) in which the magnitude–distance space is partitioned into bins of 0.2 magnitude units and 2-km distance (Fig. 9). A standard deviation of logarithmic ground-motion amplitudes was obtained if any such bin contained at least three records. Given that the purpose of pure error analysis is to obtain an estimate of the variability of ground motions resulting from a repeated scenario, smaller bin sizes were chosen (0.1 magnitude and 1-km distance increments). This trial necessarily led to fewer bins having at least three records and consequently resulted in the estimate of the magnitude dependence being based upon fewer data points. The next trial was to consider the influence of increasing the number of records required to calculate the standard deviation for a bin. Values of four and five records were chosen for this purpose, and while this re-

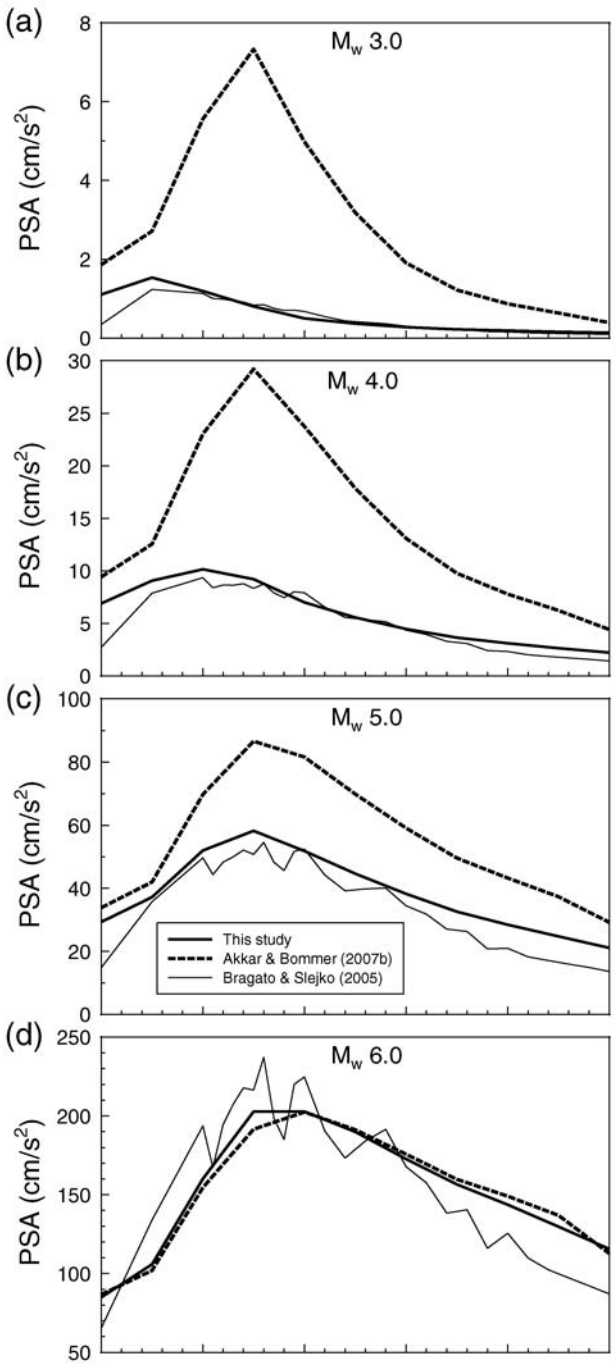

Figure 7. Comparison of predicted median spectra on stiff-soil sites at 25 km for different magnitudes from the new equations, thick lines; those of Akkar and Bommer (2007b), dashed lines; and those of Bragato and Slejko (2005), thin lines. (*Continued*)

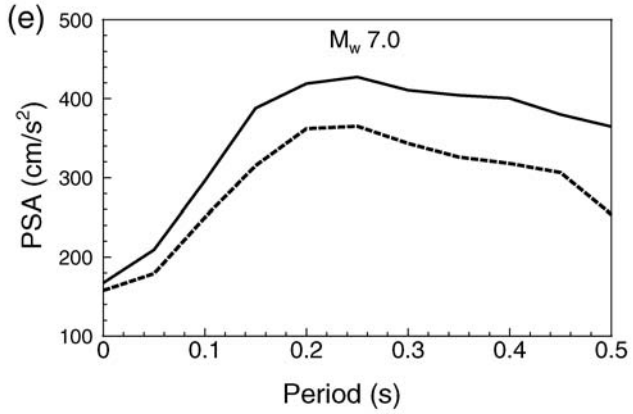

Figure 7. Continued.

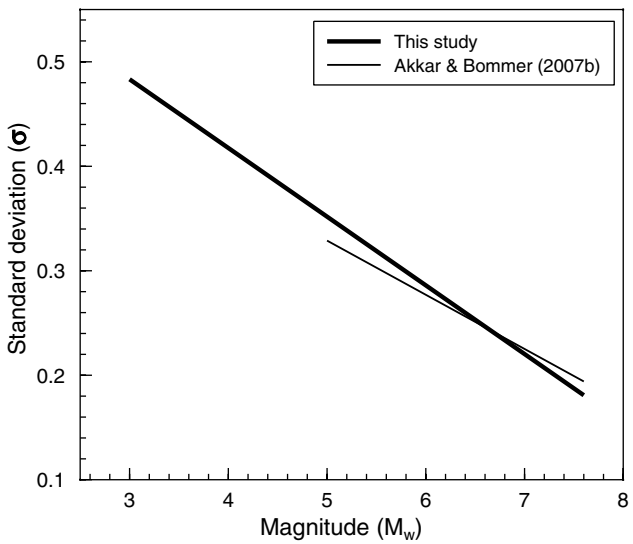

Figure 8. Comparison of magnitude-dependent sigma values for PGA from Akkar and Bommer (2007b) and the present study.

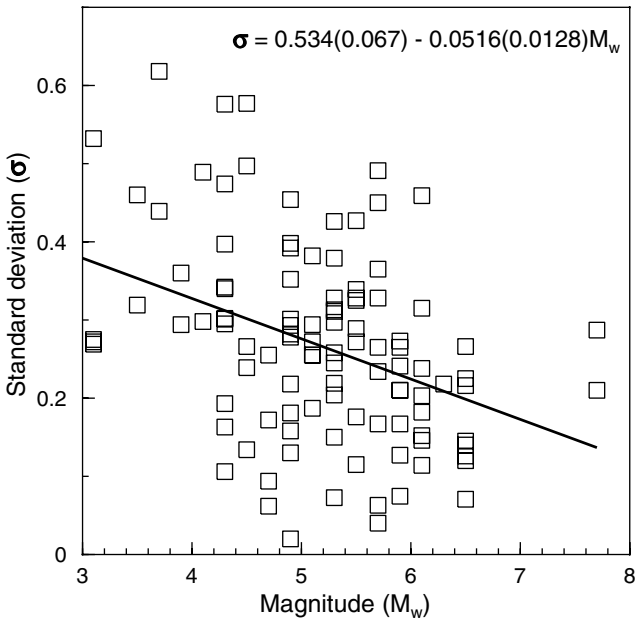

Figure 9. Magnitude dependence of the extended dataset for PGA as implied by pure error analysis using 0.2 unit magnitude and 2-km distance increments and using at least three records to obtain the standard deviation shown for each point. The coefficients of the equation, together with standard error estimates in parentheses, are present in the legend.

sulted in an increase in the confidence associated with the values of the standard deviations determined for any given bin, these are still very small samples from which to obtain a robust estimate of the variability.

An additional trial was conducted whereby logarithmic rather than linear distance increments were used. As shown earlier in this article, and by numerous others previously, the magnitude and distance dependence of ground-motion amplitudes may be well modeled using a functional form as given in equation (1). Given this *a priori* knowledge one may anticipate that the adopted binning scheme used for the pure error analysis may lead to an apparent magnitude dependence even if the data is in reality homoscedastic. Consider the partial derivatives of equation (1) with respect to both magnitude and distance as shown in equations (2) and (3), respectively:

$$\frac{\partial \log_{10}[\mathrm{PSA}(T)]}{\partial M_{\mathrm{w}}} = b_2 + 2b_3 M_{\mathrm{w}} + b_5 \log_{10} \sqrt{R_{jb}^2 + b_6^2}, \tag{2}$$

$$\frac{\partial \log_{10}[\mathrm{PSA}(T)]}{\partial R_{jb}} = \frac{(b_4 + b_5 M_{\mathrm{w}}) R_{jb}}{\ln(10)(R_{jb}^2 + b_6^2)}. \tag{3}$$

From inspection of equation (2), one can appreciate that the difference in ground-motion amplitudes across any given linear increment in magnitude, for a given distance, should decrease as the magnitude increases because b_2 is positive while b_3 is negative. Similarly, inspection of equation (3) shows that the difference in ground-motion amplitudes for any given linear increment in distance, for a given magnitude, also varies with respect to distance and that, with the exception of the near-source region, the difference reduces with increasing distance. The implication of these simple considerations is that, even if the data were truly homoscedastic, one would observe larger variation in ground-motion amplitudes for smaller events at closer distances than for larger events at larger distances. The fact that most strong-motion datasets have an inherent magnitude–distance correlation whereby a greater number of larger events are recorded at large distances simply acts to exacerbate this effect.

Figure 10 shows the results of a series of different binning schemes. While the influence of using logarithmic distance increments is not as pronounced as anticipated, an effect can nonetheless be observed. What is most significant when considering this figure is that the strength of the magnitude dependence varies greatly depending upon the binning scheme adopted. It is also noteworthy that none of these slope values are found to be statistically significant at the 95% confidence level. This is largely a result of having such unstable estimates of the standard deviation for any given bin. It can be concluded that while pure error analysis may provide some insight into the nature of ground-motion variability, current strong-motion datasets are still far too sparsely populated to enable reliable results to be obtained using this method. In light of the preceding findings new coefficients for equation (1) were determined assuming that the aleatory variability is homoscedastic; the coefficients, however, are not presented here because the main focus of this study is to reproduce the analysis of Akkar and Bommer (2007b), with heteroscedastic scatter, using an extended dataset.

Figure 11 compares the median predictions from the heteroscedastic and homoscedastic equations, from which it can be seen that they are, as would be expected, very similar, although the latter equation captures an apparently weaker nonlinear magnitude scaling and even lower magnitude dependence of the attenuation with distance. The concern that arises, however, is that even with the homoscedastic model, the sigma value is large compared to most equations in current use, and this may be problematic because the values remain high for the larger earthquake magnitudes that drive probabilistic seismic hazard analyses.

The findings of the pure error analysis suggest that while there is some magnitude dependence this dependence may not be statistically significant. However, when making the assumption of homoscedasticity, the weak magnitude dependence of the ground-motion variability that was observed during the pure error analysis still exists. The net effect is to make the magnitude scaling steeper and consequently cause the homoscedastic case to predict higher ground motions at large magnitudes than for the heteroscedastic case.

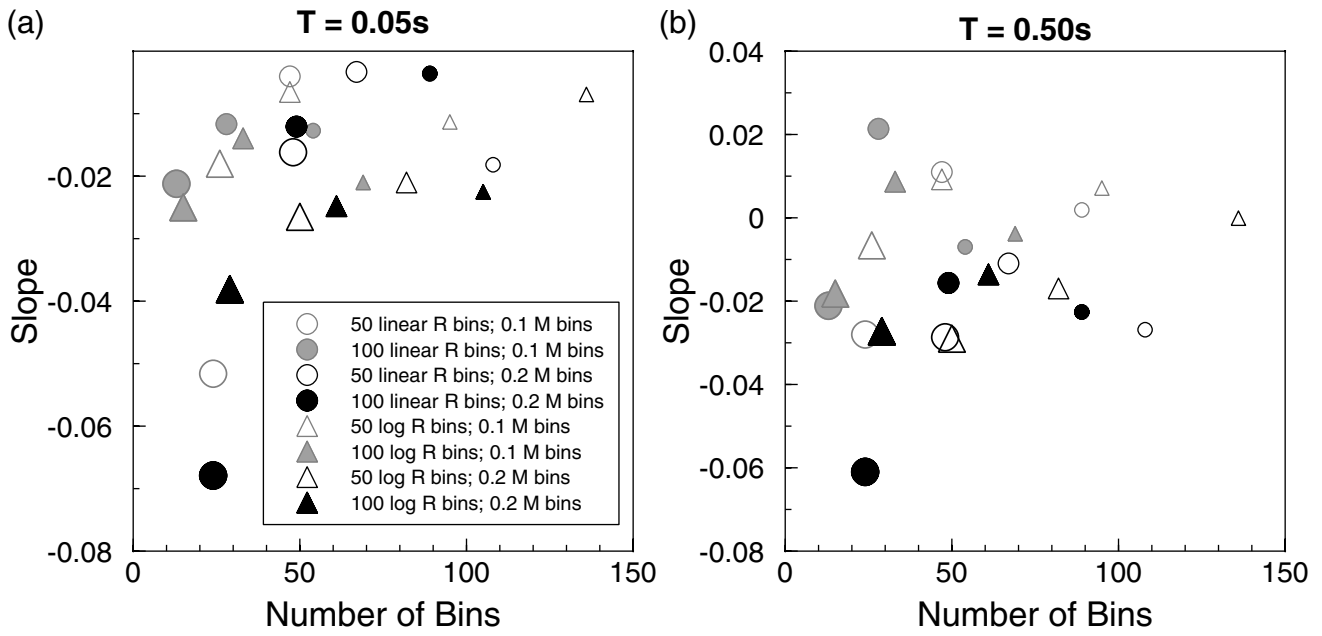

Figure 10. The influence of the binning scheme on the pure error analysis results; the ordinate shows the slope of the regression line shown in Figure 9 for a particular binning scheme. The size of the symbols corresponds to the number of data points required for the bin to be included in the pure error analysis, values being 3, 4, or 5.

Although the preceding analysis shows that there may not be an unambiguous case for a heteroscedastic model, there is no doubt that the inclusion of the small-magnitude data has resulted in a significantly increased aleatory variability. Figure 12 shows the ratios of the inter- and intraevent standard deviations from homoscedastic equations derived with the full extended dataset and another set of equations derived using the records for only M_w 5 and greater events as used by Akkar and Bommer (2007b). The plot shows unequivocally that the increased variability in the equations for the extended magnitude range comes almost entirely from increased interevent variability; this result is consistent with the findings of Youngs *et al.* (1995) that the magnitude dependence of sigma is greater for inter- than for intraevent components. This could very easily be the result of greater uncertainty in the determination of moment magnitudes and other parameters for the smaller earthquakes. That the lower reliability of the small-magnitude metadata may be responsible for the increase in the interevent variability is also supported by the findings of Rhoades (1997), in which it was demonstrated that through accounting for the uncertainties in magnitude estimates a marked reduction in the interevent variability can be achieved.

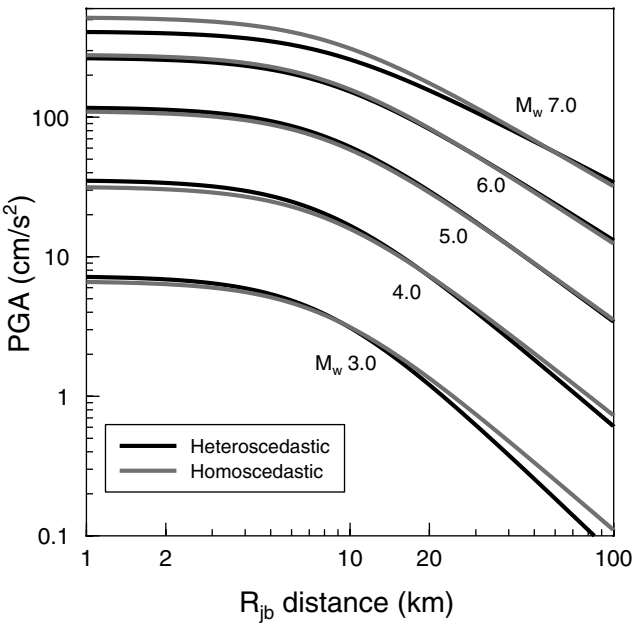

Figure 11. Comparison of predicted median values of PGA for strike-slip ruptures and rock sites from the heteroscedastic and homoscedastic equations for various combinations of magnitude and distance.

In this respect it is also interesting to note that although many of the ground-motion prediction equations in use in western North America during the last decade did have magnitude-dependent variability, most of the models emerging from the Next Generation of Attenuation (NGA) project (Boore and Atkinson, 2007; Campbell and Bozorgnia, 2007; Chiou and Youngs, 2006) have constant standard deviations, leading analysts to conclude that the previously encountered heteroscedastic variability was in fact a result of uncertainties in the metadata for smaller events (Campbell and Bozorgnia, 2007).

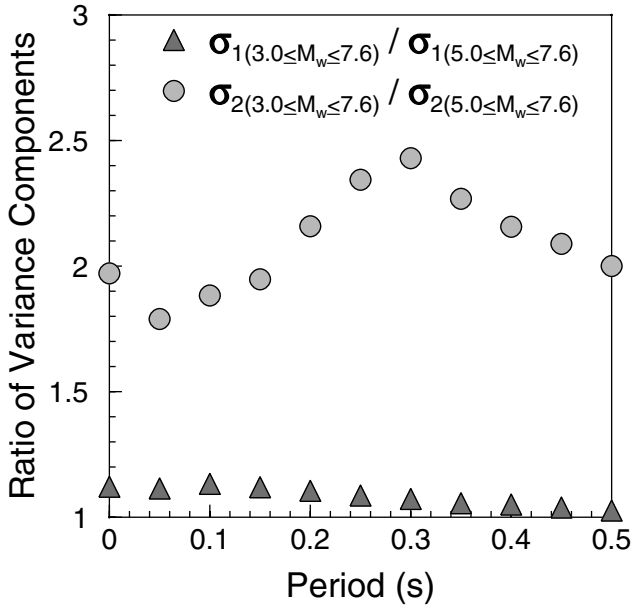

Figure 12. Ratios of interevent (σ_2) and intraevent (σ_1) standard deviations from homoscedastic equations derived using the full dataset from M_w 3 to 7.6 and only events of M_w 5 and greater.

One possible cause of the increased variability for the extended dataset may be the combination of data from several different regions (some operating different instruments) and the fact that ground motions from smaller earthquakes may be more sensitive to differences in crustal structure. In order to explore this possibility, the regressions were repeated removing the data from events smaller than M_w 5 from each of the four regions contributing significantly to the small-magnitude data. The resulting equations and associated standard deviations for PGA and PSA[0.25] are compared with each other and with heteroscedastic equations obtained using the whole dataset in Figure 13. The plots clearly indicate that the median motions and their variability are not sensitive to the inclusion of any of these individual regional datasets.

To investigate further any possible regional differences, the inter- and intraevent residuals for the four equations obtained with regional subsets of small-magnitude data removed are plotted against earthquake magnitude (Fig. 14). It should be noted that *sensu stricto* these are not true residuals as the plotted data points by definition were not included in the regression analysis. The split into inter- and intraevent residuals has therefore been made by assuming that the inter- and intraevent standard deviations that were obtained from the regression on the dataset excluding these points are valid for these points also. The residuals do not show any clear deviations from the general trend of the complete dataset, with the possible exception of the Spanish subset; however, because this is also the smallest regional subset, the inclusion of this data is not likely to explain the increased standard deviation for the equations derived from the extended magnitude range.

Is there Evidence for Soil Nonlinearity?

A possible limitation of the equations derived using equation (1) is that it does not include soil nonlinearity. Akkar and Bommer (2007a) examined the residuals of PGV in each site class against the predicted value in order to explore evidence for nonlinear soil response but found no significant trends. The residuals of the new equations are analyzed in a similar way to search for soil nonlinearity; Figure 15 shows the soft-soil site residuals of PGA, although the same patterns are observed across the spectrum.

The plots in Figure 15 show the full datasets and, on the right-hand side, only those for the stronger rock motions because evidence of nonlinearity is expected to become apparent only for accelerations beyond 100–200 cm/sec^2 (Beresnev and Wen, 1996). The plots are shown for the total residuals and for the intraevent residuals, because the latter should be expected to more clearly reveal such site effects if they are present. Although there are trend lines fitted through the data on the right-hand side of the plot with a negative slope, as would be expected, the slope is very mild—especially for the intraevent residuals—and poorly constrained. The only conclusion that can be drawn is that the data does not provide a robust model that would allow an adjustment to be made for soil nonlinearity.

Soil nonlinearity is a well-established and broadly recognized phenomenon and has been included in recent ground-motion prediction equations such as the preliminary models of the NGA project cited previously. However, there are many reasons why soil nonlinearity may not be apparent even when considering an extended range of ground-motion amplitudes. For a start, the site classification scheme that is adopted in this work must be regarded as being a relatively crude attempt to account for the influence of near-surface geology when predicting ground motions. The types of sites that are grouped together into any given class vary significantly from one to another. In most cases the site class is based upon the average shear-wave velocity over the upper 30 m. However, the range of shear-wave velocity that is associated with each site class is large, and the 30 m limit is an arbitrary criterion to characterize the properties of the near-surface geological profile. In addition, when plotting the residuals against the median prediction for rock, one is dealing with uncorrelated ground motions, that is, the prediction on rock is simply the median estimate of the ground motion for the same magnitude, distance, and style-of-faulting scenario and is not the actual ground motion on rock at the site. With the current dataset, as revealed in Figure 15, there is also the serious limitation that there are very few recordings at soil sites with high amplitudes, whence there are very few data for which nonlinearity would have been strongly invoked so that the influence could be revealed through examination of residuals.

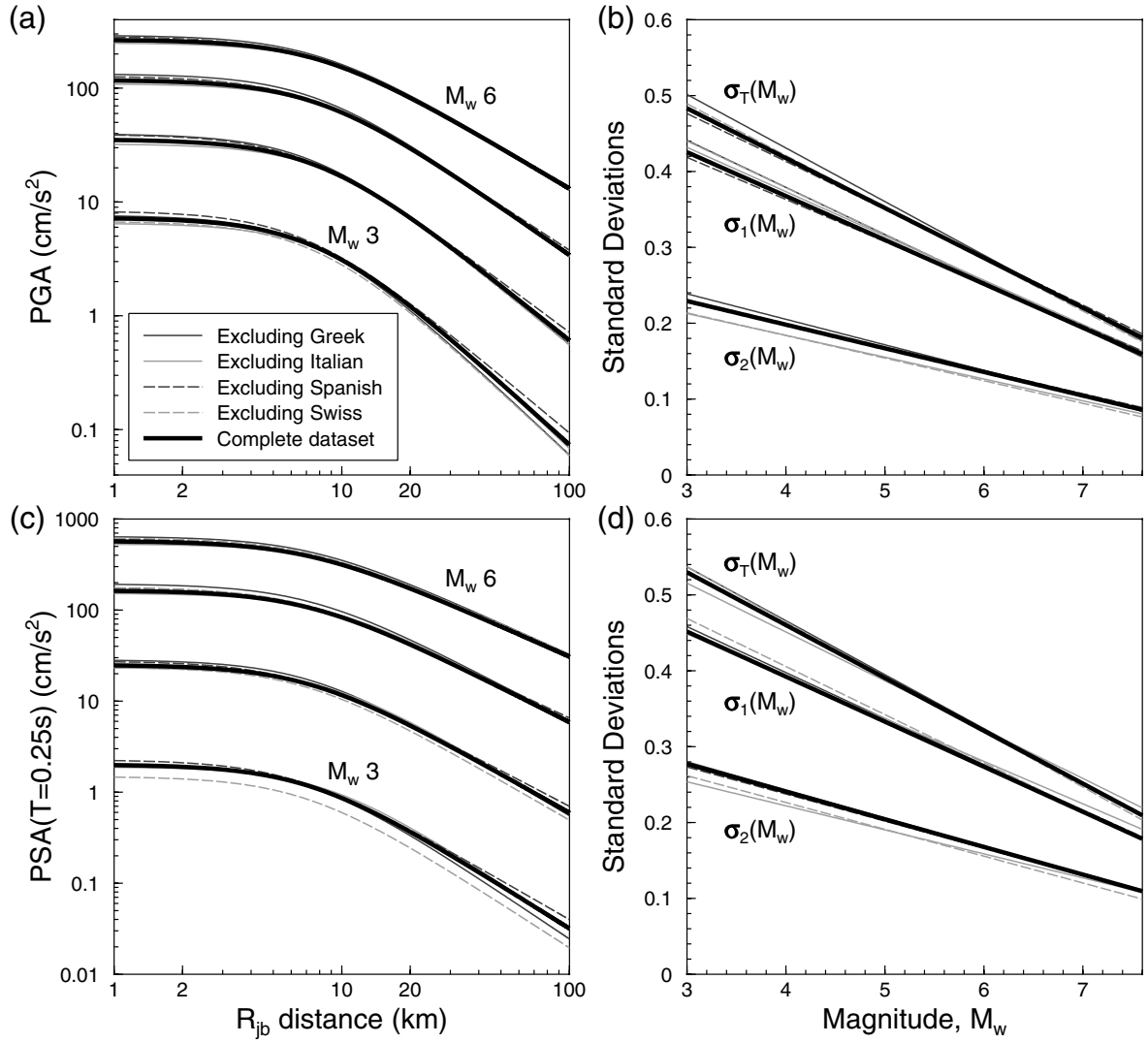

Figure 13. (a) Predicted median values of PGA; (b) standard deviations for PGA; (c) predicted median values of PSA[0.25 sec]; and (d) standard deviations for PSA[0.25 sec]. All plots are for strike-slip ruptures and rock sites from the original equations and those obtained excluding the small-magnitude data from four countries.

Therefore, while the predictive model proposed herein does not include terms to account for the larger soil amplification of weak motions than of large, as is expected for nonlinear site response, this should not be taken as evidence against soil nonlinearity. Rather this leads to the conclusion that the soil classification scheme currently used for the development of European predictive equations must be improved and more genuinely strong recordings are needed before soil nonlinearity may be reliably modeled for this region.

Discussion

This article has presented new equations for the prediction of short-period response spectral ordinates in Europe and the Middle East using a dataset that extends the data used by Akkar and Bommer (2007b) from a lower magnitude limit of M_w 5 to M_w 3. The functional form and fitting procedures followed in deriving the new equations are identical to those employed by Akkar and Bommer (2007b). This prompts, before drawing definitive conclusions, exploration of whether this approach is appropriate over such a wide magnitude range. Inspection of Figures 4 and 5, comparing the equations of Akkar and Bommer (2007b) and that for the extended magnitude range presented herein, shows that the magnitude scaling, as indicated by the misfit at small distances, of the two equations is significantly different. The new equation predicts lower ground motions for smaller magnitudes, which is to be expected, but interestingly also predicts higher ground motions at larger magnitudes. A prudent question that should therefore be asked is whether or not the quadratic magnitude scaling adopted in this study is sui-

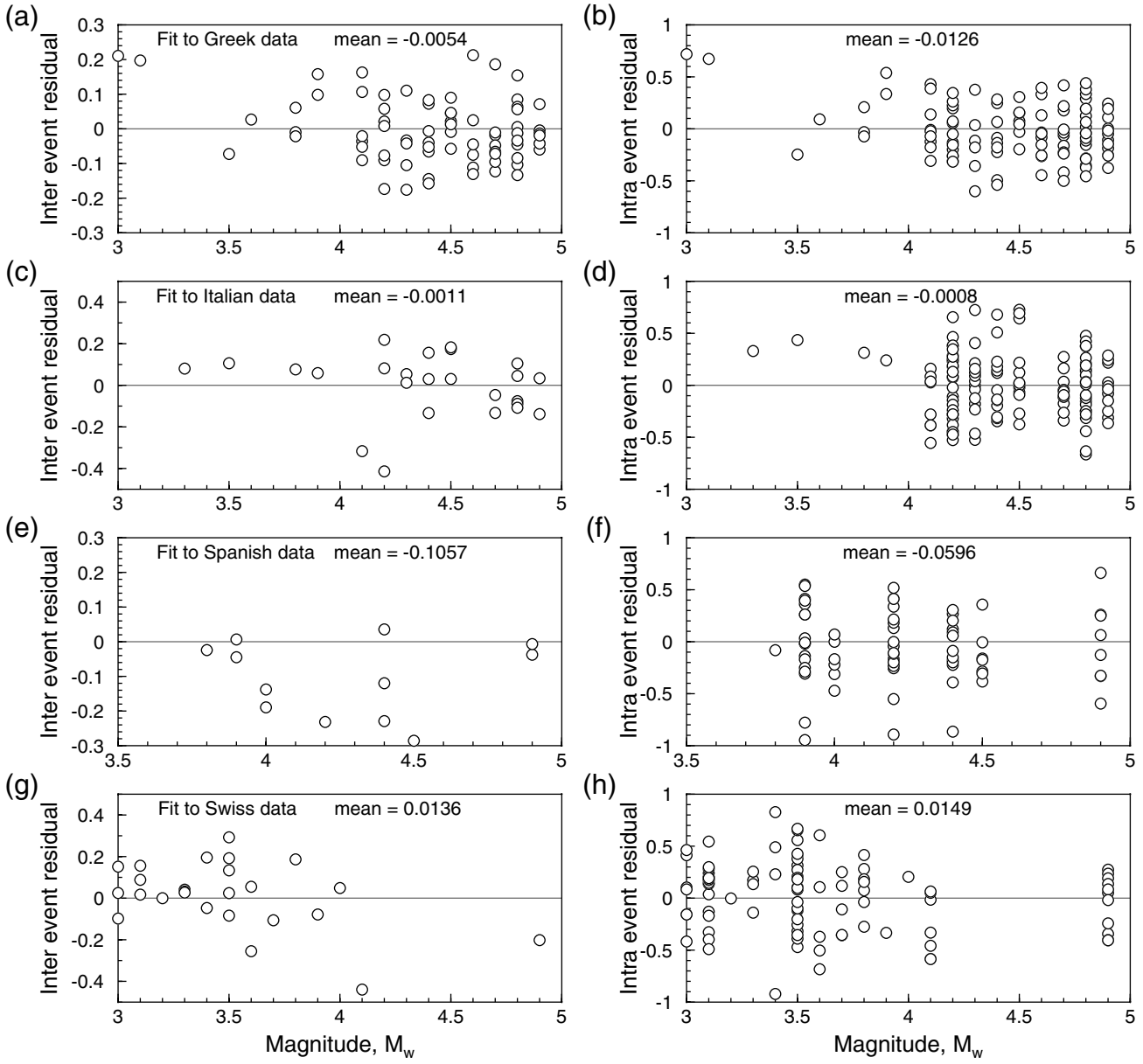

Figure 14. Inter- and intraevent residuals calculated for small-magnitude data from four countries using PGA equations derived with these data excluded from the regressions.

table for application over the entire extended magnitude range. As a first step in attempting to address this question, plots of both inter- and intraevent residuals were generated that indicated that the functional form is performing well over the entire magnitude range (Fig. 16). However, the new equations are derived only for the purpose of exploring the effect of the extended magnitude range and are not proposed for application.

The critical parameters that govern the magnitude scaling are b_2 and b_3, so it is therefore instructive to consider the values of these terms derived for the two different magnitude ranges. In doing so, one finds that the values of b_3 are relatively similar for the two datasets and that the major difference occurs in the values of b_2, where these values are significantly larger for the extended magnitude dataset. This comparison suggests that the effect of adding additional small-magnitude data is to steepen the magnitude scaling. As the values of b_3 are similar for the two datasets, the linear portion of the magnitude scaling, for small magnitudes, is constrained by more data, and the second-order term is not strong enough to sufficiently flatten the magnitude scaling off at higher magnitudes—hence the reason for the larger predictions at large magnitudes. While the residual plot indicates that the magnitude scaling over the larger magni-

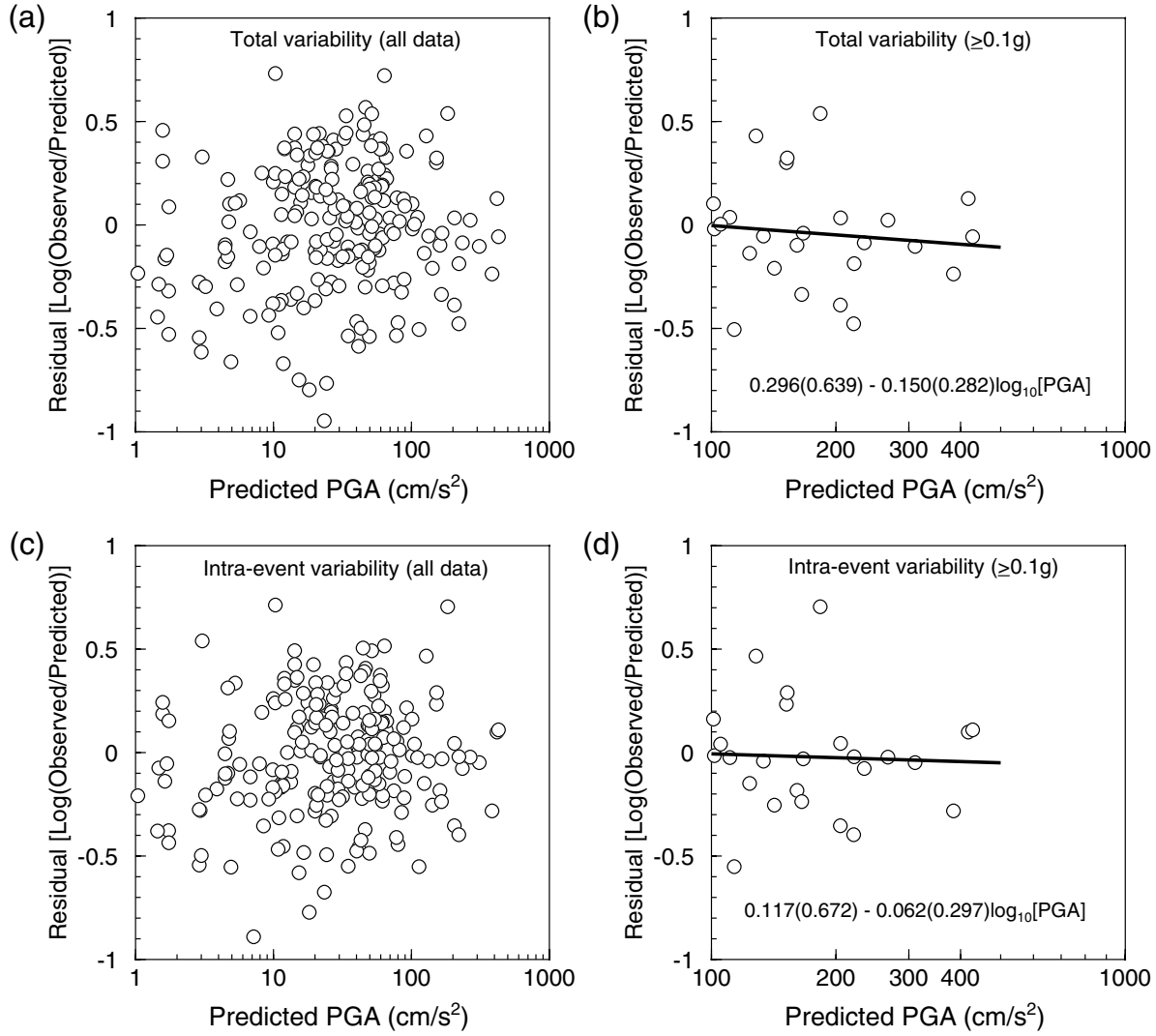

Figure 15. Residuals for soft-soil sites plotted against predicted rock PGA; the plots on the right show only the data for predicted peak accelerations above 0.1g. Equations for trends of these residuals with respect to PGA > 0.1g (with associated standard error estimates of coefficients in parentheses) are given in the right-hand plots.

tudes is still sound, it may be that this effect is being disguised by the complex interplay between the inter- and intraevent residuals.

Recently, the researchers within the NGA project have proposed various alternatives to the traditional continuous magnitude scaling. Chiou and Youngs (2006) have demonstrated that it is possible to account for different magnitude scaling above and below the corner frequency. While the magnitude scaling of their model appears relatively complicated, it may be very well approximated by a continuous quadratic function as done in the present work. Boore and Atkinson (2007) employ quadratic magnitude scaling but conduct their regression analysis such that their model prevents over-saturation from occurring; that is, the b_3 term cannot be so strong that predicted ground motions start to decrease with increasing magnitude. Idriss (2007) and Campbell and Bozorgnia (2007) adopt bilinear and trilinear magnitude scaling, respectively. In effect, all of the NGA models proposed thus far attempt to capture the same effect: linear scaling for small-to-moderate sized earthquakes with a progressive fall-off in slope with increasing magnitude. Although our model for the extended magnitude range is in accord with these state-of-the-art models, it is probable that an improved approach to modeling the magnitude scaling over a very extended range would be to constrain the magnitude scaling to be linear at low magnitudes and then allow for a quadratic (or similar) fall-off in slope over the upper magnitude ranges. However, the clear absence of any distinct trend in the residuals shown in the upper frames of Figure 16 suggests that for the M_w 3.0–7.6 dataset used in this study, the quadratic scaling model appears to be perfectly adequate to capture the dependence of ground-motion

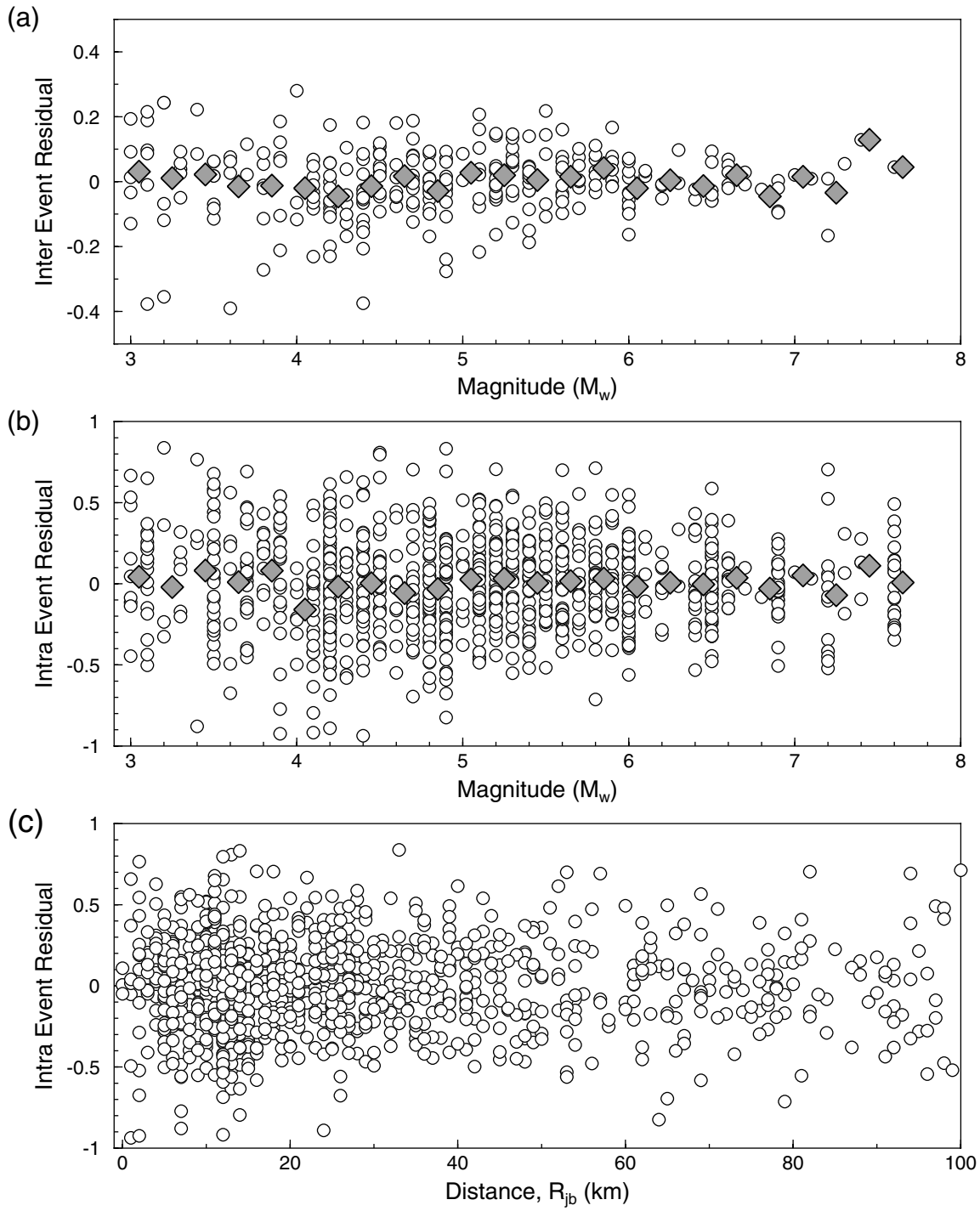

Figure 16. Inter- and intraevent residuals from the heteroscedastic model for PGA (Tables 2 and 3) against magnitude and distance. For the residuals plotted against magnitude, the mean value of the residuals in bins of 0.2 M_w are indicated by diamonds.

amplitudes on earthquake magnitude. The advantages, in terms of application, of a single model for the full range of magnitudes are obvious.

One clear result of the analyses presented in this article is the very strongly nonlinear magnitude scaling of ground-motion amplitudes and the comparatively weak magnitude dependence of the attenuation. In this respect it does need to be borne in mind that in our extended dataset there are very few data from small-magnitude events recorded at large distances (> 50 km) (possibly in part due to censoring as a result of nontriggering of instruments). This means that the attenuation over the full distance range is governed to a sig-

nificant extent by the recordings of larger earthquakes. However, it may also be the case that the attenuation is not in fact strongly dependent on magnitude and functional forms assuming such a dependence may actually be capturing a source-related effect, whereby b_6 in equation (1) should in fact be magnitude dependent.

Conclusions

The most important conclusion from this study, which is not new but adds more support to what is becoming widely acknowledged, is that empirical ground-motion prediction equations should not be used for estimating spectral ordinates for earthquakes of magnitudes outside the range of the dataset on which they are derived. An even more interesting finding is that it would appear that equations are not limited only in applicability to the magnitude range on which they are based but may also be unreliable at the limiting values of magnitude. For the lower magnitude limit considered in PSHA calculations, the solution is relatively simple, and equations simply need to be derived including records from events of about one magnitude unit below this limit, notwithstanding that this may be problematic for longer-period spectral ordinates. At the upper limit of magnitude considered in PSHA calculations, which in general is already in excess of the largest magnitude represented in the datasets used to derive empirical prediction equations, the problem is more serious. Estimates of epistemic uncertainty in ground-motion prediction for large-magnitude events may need to be broadened to take account of this finding, although seismological modeling may be able to provide constraints on the larger-magnitude motions.

The strongly nonlinear magnitude dependence of ground-motion amplitudes shown by the results presented herein challenges claims that small-magnitude data have revealed pronounced regional differences in ground-motion prediction. Indeed, only very small regional differences in the small-magnitude data were identified in this study, and these cannot be decoupled from the distributions of these small datasets. One could argue that it would not be unreasonable to conclude that if small-magnitude recordings from a given region were well matched by the new equations for an extended magnitude range, the equations derived for larger earthquakes would be applicable in PSHA within those regions.

If empirical ground-motion prediction equations are to be used in PSHA, for which lower magnitude limits close to M_w 5 are usually adopted, the results of this study suggest that the equations should be derived using recordings from events at least as small as M_w 4. A consequence of incorporating small-magnitude data is that the aleatory variability of the equations is greatly increased. The results of sensitivity studies suggest that the magnitude dependence found in previous studies of European ground motion may primarily reflect a magnitude–distance correlation in the datasets in combination with less than optimal binning schemes used for the pure error analysis. However, the results also show unequivocally that including the additional data from small-magnitude earthquakes, while assuming homoscedastic variability, leads to a large increase in the value of sigma. This may well be due to greater uncertainty in the metadata associated with the smaller-magnitude earthquakes, and further work needs to be done on this issue.

The equations presented in this study are not proposed for application, because the purpose was only to explore the effect of extending the magnitude range. The next phase of work will be to derive new European equations for a wide magnitude range, which may involve the use of alternative functional forms and possibly alternative fitting techniques; the importance of the style of faulting, for example, is unlikely to be meaningful for small events that can be approximated as point sources for most recording locations. The first stage of the work must be a careful inspection and processing of the strong-motion data and a systematic reevaluation of the magnitudes and distances on a homogeneous basis (Douglas, 2003b).

Acknowledgments

We thank Fleur Strasser for her assistance with the preparation of the small-magnitude data and John Douglas for the use of his regression software. We are also very grateful to Ellen Rathje for interesting and informative discussions regarding the exploration of soil nonlinearity.

We are very grateful to Frank Scherbaum, Graeme McVerry, and an anonymous reviewer for insightful evaluations of the manuscript and very useful and constructive suggestions, which we believe appreciably improved the article. Suggestions by Ivan Wong improved the final version of the article.

We would also like to thank various sponsors whose generous financial support has made this work possible: Peter Stafford is a Research Fellow of the Willis Research Network; John Alarcón is partially funded by the Alβan program of the European Union; and Sinan Akkar was able to visit Imperial College London to initiate this work with the assistance of TUBITAK and the Royal Society.

References

Abrahamson, N. A., and K. M. Shedlock (1997). Overview, *Seism. Res. Lett.* **68,** 9–23.

Akkar, S., and J. J. Bommer (2006). Influence of long-period filter cut-off on elastic and inelastic spectral displacements, *Earthq. Eng. Struct. Dyn.* **35,** 1145–1165.

Akkar, S., and J. J. Bommer (2007a). New empirical prediction equations for peak ground velocity derived from strong-motion records from Europe and the Middle East, *Bull. Seismol. Soc. Am.* **97,** no. 2, 511–530.

Akkar, S., and J. J. Bommer (2007b). Prediction of elastic displacement response spectra in Europe and the Middle East, *Earthq. Eng. Struct. Dyn.* **36,** 1275–1301.

Ambraseys, N. N., K. A. Simpson, and J. J. Bommer (1996). The prediction of horizontal response spectra in Europe, *Earthq. Eng. Struct. Dyn.* **25,** 371–400.

Ambraseys, N. N., J. Douglas, S. K. Sarma, and P. M. Smit (2005). Equations for the estimation of strong ground motions from shallow crustal earthquakes using data from Europe and the Middle East: horizontal peak ground acceleration and spectral acceleration, *Bull. Earthq. Eng.* **3,** 1–53.

Ambraseys, N. N., P. Smit, J. Douglas, B. Margaris, R. Sigbjörnsson, S. Ólafsson, P. Suhadolc, and G. Costa (2004). Internet site for European strong-motion data, *Boll. Geofis. Teor. Appl.* **45,** 113–129.

Beresnev, I. A., and K. L. Wen (1996). Nonlinear soil response—a reality?, *Bull. Seismol. Soc. Am.* **86,** 1964–1978.

Beyer, K., and J. J. Bommer (2006). Relationships between median values and aleatory variabilities for different definitions of the horizontal component of motion, *Bull. Seismol. Soc. Am.* **96,** 1512–1522.

Bommer, J. J., J. Douglas, and F. O. Strasser (2003). Style-of-faulting in ground motion prediction equations, *Bull. Earthq. Eng.* **1,** 171–203.

Bommer, J. J., G. Georgallides, and I. J. Tromans (2001). Is there a near-field for small-to-moderate magnitude earthquakes?, *J. Earthq. Eng.* **5,** 395–423.

Bommer, J. J., S. Oates, J. M. Cepeda, C. Lindholm, J. F. Bird, R. Torres, G. Marroquín, and J. Rivas (2006). Control of hazard due to seismicity induced by a hot fractured rock geothermal project, *Eng. Geol.* **83,** 287–306.

Boore, D. M., and G. M. Atkinson (2007). PEER Report 2007/01: Boore–Atkinson NGA ground motion relations for the geometric mean horizontal component of peak and spectral ground motion parameters, Pacific Earthquake Engineering Research Center, Berkeley, CA, 234 pp.

Bragato, P. L., and D. Slejko (2005). Empirical ground-motion attenuation relations for the eastern Alps in the magnitude range 2.5–6.3, *Bull. Seismol. Soc. Am.* **95,** 252–276.

Campbell, K. W., and Y. Bozorgnia (2007). PEER Report 2007/02: Campbell–Bozorgnia NGA ground motion relations for the geometric mean horizontal component of peak and spectral ground motion parameters, Pacific Earthquake Engineering Research Center, Berkeley, CA, 240 pp.

Chiou, B. S.-J., and R. R. Youngs (2006). Chiou and Youngs PEER-NGA empirical ground motion model for the average horizontal component of peak acceleration and psuedo-spectral acceleration for spectral periods of 0.01 to 10 seconds, Interim Reports of Next Generation Attenuation (NGA) Models, interim report for U.S. Geol. Surv. review, 14 June 2006 (revised 10 July 2006), Richmond, California, Pacific Earthquake Engineering Research Center, 219 pp.

Cotton, F., F. Scherbaum, J. J. Bommer, and H. Bungum (2006). Criteria for selection and adjusting ground-motion models for specific target regions: application at Central Europe and rock sites, *J. Seism.* **10,** 137–156.

Dost, B., T. van Eck, and H. Haak (2004). Scaling of peak ground acceleration and peak ground velocity recorded in The Netherlands, *Boll. Geofis. Teor. Appl.* **45,** 153–168.

Douglas, J. (2003a). Earthquake ground motion estimation using strong-motion records: a review of equations for the estimation of peak ground accelerations and response spectral ordinates, *Earth Sci. Rev.* **61,** 43–104.

Douglas, J. (2003b). A note on the use of strong-motion data from small magnitude earthquakes for empirical ground motion estimation, in *Skopje Earthquake 40 Years of European Earthquake Engineering SE-40EEE*, August, Skopje/Ohrid, Macedonia, Institute of Earthquake Engineering and Engineering Seismology.

Douglas, J., and P. J. Smit (2001). How accurate can strong ground motion attenuation relations be?, *Bull. Seismol. Soc. Am.* **91,** 1917–1923.

Frisenda, M., M. Massa, D. Spallarossa, G. Ferretti, and C. Eva (2005). Attenuation relationship for low magnitude earthquakes using standard seismometric records, *J. Earthq. Eng.* **9,** 23–40.

Idriss, I. M. (2007). Empirical model for estimating the average horizontal values of pseudo-absolute spectral accelerations generated by crustal earthquakes, Volume 1 sites with $Vs30 = 450$ to 900 m/s, Interim Reports of Next Generation Attenuation (NGA) Models, interim report issued for U.S. Geol. Surv. review, 19 January 2007, Richmond, California, Pacific Earthquake Engineering Research Center, 76 pp.

Marin, S., J. P. Avouac, N. Marc, and A. Schlupp (2004). A probabilistic approach to seismic hazard in Metropolitan France, *Bull. Seismol. Soc. Am.* **94,** 2137–2163.

Rhoades, D. A. (1997). Estimation of attenuation relations for strong-motion data allowing for individual earthquake magnitude uncertainties, *Bull. Seismol. Soc. Am.* **87,** 1674–1678.

Scherbaum, F., F. Cotton, and P. Smit (2004). On the use of response spectral reference data for the selection of ground-motion models for seismic hazard analysis: the case of rock motions, *Bull. Seismol. Soc. Am.* **94,** 2164–2185.

Theodulidis, N. P. (1998). Peak ground acceleration attenuation of small earthquakes: analysis of Euroseistest, Greece, data, *The Effects of Surface Geology on Seismic Motion*, K. Irikura, K. Kudo, H. Okada and T. Sasatani (Editors), Balkema, Rotterdam, The Netherlands, 1171–1176.

van Eck, T., F. Goutbeek, H. Haak, and B. Dost (2006). Seismic hazard due to small-magnitude, shallow-source induced earthquakes in The Netherlands, *Eng. Geol.* **87,** 105–121.

Youngs, R. R., N. A. Abrahamson, F. I. Makdisi, and K. Sadigh (1995). Magnitude-dependent variance of peak ground acceleration, *Bull. Seismol. Soc. Am.* **85,** 1161–1176.

Civil and Environmental Engineering Department
Imperial College London
South Kensington campus
London SW7 2AZ, United Kingdom
(J.J.B., P.J.S., J.E.A.)

Earthquake Engineering Research Center
Civil Engineering Department
Middle East Technical University
06531 Ankara, Turkey
(S.A.)

Manuscript received 2 April 2007